Available online at www.sciencedirect.com
SCIENCE DIRECT
International Journal of Pharmaceutics 314 (2006) 21–30
INTERNATIONAL JOURNAL OF PHARMACEUTICS
www.elsevier.com/locate/ijpharm

Modelling intestinal absorption of salbutamol sulphate in rats

B. Valenzuela [a,*], E. López-Pintor [a], J.J. Pérez-Ruixo [a,b], A. Nácher [c], A. Martín-Villodre [c], V.G. Casabó [c]

[a] *Pharmacy and Pharmaceutics Division, Department of Engineering, Faculty of Pharmacy, Miguel Hernández University, Crta. Alicante-Valencia km. 87, 03550 San Juan de Alicante, Alicante, Spain*
[b] *Clinical Pharmacology and Experimental Medicine Division, Johnson & Johnson Pharmaceutical Research & Development, a Division of Janssen Pharmaceutica NV, Belgium, Turnhoutseweg, 30 2340 Beerse, Belgium*
[c] *Department of Pharmacy and Pharmaceutics, Faculty of Pharmacy, University of Valencia, Avda. Vicente A. Estellés s/n, 46100 Burjassot, Valencia, Spain*

Received 23 August 2005; accepted 13 January 2006
Available online 30 March 2006

Abstract

The objective was to develop a semiphysiological population pharmacokinetic model that describes the complex salbutamol sulphate absorption in rat small intestine. In situ techniques were used to characterize the salbutamol sulphate absorption at different concentrations (range: 0.15–18 mM). Salbutamol sulphate at concentration of 0.29 mM was administered in presence of verapamil (10 and 20 mM), grapefruit juice and sodium azide (NaN_3) (0.3, 3 and 6 mM). Different pharmacokinetic models were fitted to the dataset using NONMEM. Parametric and non-parametric bootstrap analyses were employed as internal model evaluation techniques. The validated model suggested instantaneous equilibrium between salbutamol sulphate concentrations in lumen and enterocyte, and the salbutamol sulphate absorption was best described by a simultaneous passive diffusion ($k_a = 0.636\ h^{-1}$) and active absorption ($V_{Max} = 0.726$ mM/h, $K_m = 0.540$ mM) processes from intestinal lumen to enterocyte, together with an active capacity-limited P-gp efflux ($V'_{Max} = 0.678$ mM/h, $K'_m = 0.357$ mM) from enterocyte to intestinal lumen. The extent of salbutamol sulphate absorption in rat small intestine can be improved by NaN_3, grapefruit juice and verapamil.

Keywords: Salbutamol sulphate; Intestinal absorption; Active transport; Oral bioavailability; P-glycoprotein inhibitors; Kinetic modelling

1. Introduction

Salbutamol sulphate is a β-2-adrenergic agonist widely used in the treatment of asthmatic disorders and chronic obstructive lung diseases. The absolute oral bioavailability of salbutamol sulphate when administered in conventional dosage forms has shown to be incomplete, variable and rather irregular (Ahrens and Smith, 1984). An increasing number of drugs have been reported to have similar absorption profiles. In fact, HIV protease inhibitors (ritonavir, indinavir, saquinavir) or anti-cancer drugs (for instance, vinblastine, docetaxel, etc.) have been reported to have incomplete, variable and irregular absorption profiles, probably mediated by the transporters of the ATP-binding cassette family (Varma et al., 2003). Pre-systemic interactions with P-glycoprotein (P-gp) together with metabolism via intestinal sulphation have been argued as a potential explanation for salbutamol sulphate poor oral bioavailability (Pacifici et al., 1997). In two previous articles (Valenzuela et al., 2001, 2004), the absorption process of aqueous salbutamol sulphate solutions along the whole length of the rat small intestine was demonstrated to be modulated by an active secretion process of the drug from the enterocytes to the luminal fluid, probably mediated by P-gp.

Furthermore, Valenzuela et al. evaluated the effect of verapamil and sodium azide (NaN_3) in the salbutamol sulphate intestinal absorption and confirmed the involvement of P-gp in salbutamol sulphate absorption (Valenzuela et al., 2001). The ability of verapamil to inhibit P-gp was demonstrated in 1981 (Tsuruo et al., 1981) and, nowadays it is a specific P-gp inhibitor widely used in intestinal transport assays (Woodland et al., 2003). NaN_3 is a metabolic inhibitor, which affects mitochondrial oxidative phosphorylation and, therefore, it is able to impair ATP-dependent carrier systems. NaN_3 has been utilized to elucidate the transport of drugs (Legen et al., 2003), including those that are P-gp substrates (Shono et al., 2004). Lately,

* Corresponding author. Tel.: +34 965 919414; fax: +34 965 919528.
E-mail address: bvalenzuela@umh.es (B. Valenzuela).

0378-5173/$ – see front matter © 2006 Elsevier B.V. All rights reserved.
doi:10.1016/j.ijpharm.2006.01.019

the grapefruit juice, a natural P-gp inhibitor (Tanakaga et al., 1998), has been also used to investigate absorption process for P-gp substrates. However, components of grapefruit juice act not only as inhibitors of P-gp, but also as inhibitors of intestinal CYP3A4 enzyme (Edwards et al., 1996).

Population pharmacokinetic modelling has been implemented across all phases of drug development and, combined with simulation methods, provides a tool for better understanding the expected range of concentrations from competing dose administration strategies (Williams and Ette, 2000). Population pharmacokinetics methods have been applied to integrate and analyse data from preclinical studies in different animal models (Parker et al., 2001; Leal et al., 2005; Tunblad et al., 2005), including in situ studies in rats (Ruíz-Balaguer et al., 2002; Fernandez-Teruel et al., 2005; Muñoz et al., 2005).

The main objective of this study was to develop a semi-physiological population pharmacokinetic model to describe the intestinal absorption of salbutamol sulphate in rat and quantify the effect of verapamil, grapefruit juice and NaN_3 on the salbutamol sulphate absorption.

2. Methods

2.1. Absorption studies

Absorption studies were performed on male Wistar rats in standard stabling conditions, weighing 250–300 g, fasted for 24 h with free access to water and maintained in a light/dark cycle of 12/12 h. Anaesthesia was induced 1 h before surgery by an intraperitoneal injection of 40 mg/kg pentobarbital. The in situ technique using the whole small intestine in rat, described by Doluisio et al. (Doluisio et al., 1969) and modified as previously reported (Martín-Villodre et al., 1986) was used. In order to prevent enterohepatic recycling, the bile duct was cannulated prior to the drug perfusion. The proximal end of the small intestine was also cannulated and the intestinal lumen was cleaned with 200 mL saline in order to remove faeces.

Salbutamol sulphate (Laboratorios Aldo-Union, Barcelona, Spain) was dissolved in saline solution at concentrations of 0.15, 0.29, 1.20, 5.0, 9.0, 13.0 and 18.0 mM. Solutions were buffered to 6.4 by addition of 1% (v/v) phosphate solutions in order to reproduce the intestinal lumen pH conditions. For each concentration, 10 mL of the solution were perfused in the whole small intestine of eight rats at 37 °C. In addition, 10 mL of a 0.29 mM salbutamol sulphate solution were perfused to (1) two groups of eight rats in the presence of verapamil (Laboratorios Sigma, Barcelona, Spain) solution at concentrations of 10 and 20 mM; (2) one group of eight rats in the presence of grapefruit juice, diluted 50% (v/v); (3) three groups of eight rats in the presence of NaN_3 (Laboratorios Sigma, Barcelona, Spain) solution at concentrations of 0.3, 3.0, or 6.0 mM. All solutions prepared were isotonized before administration.

All pharmacokinetic studies and procedures described in this paper were approved by the Research Committee of Animal Use of the Faculty of Pharmacy of Valencia (Spain) and performed according to the "Principles of Laboratory Animal Care" and the European guidelines described in the EC Directive 86/609.

2.2. Water reabsorption studies

Since the reduction in the volume of the perfused solutions at the end of the experiments was significant (between 13 and 33%), in order to calculate the absorption rate constants accurately a concentration correction became necessary. Water reabsorption was characterized as an apparent zero order process (Martín-Villodre et al., 1986; Gabús-Sannié and Buri, 1987). A model based on direct measurement of the remaining volume of the test solution was employed (Sancho-Chust et al., 1995). The volume at the beginning of the experiment (V_0) for each compound was determined in grups of three animals, while the volume at the end (V_t) was measured in every animal. The sample concentration of each time-point, C_e was corrected as follows:

$$C = C_e \frac{V_t}{V_0} \quad (1)$$

where C represents the concentration in the gut that would exist in the absence of the water reabsorption process at time t. The C values over the time of the assay were used to calculate the apparent absorption rate constant.

2.3. Sampling schedule and analytical methods

In each rat, 200 μL samples were withdrawn to measure the remaining salbutamol sulphate concentrations in the intestinal lumen at 5, 10, 15, 20, 25 and 30 min from the end of the perfusion. Salbutamol sulphate levels were measured by a high-performance liquid chromatographic method previously described (Valenzuela et al., 2001). This method had a limit of quantification of 0.1 μM and excellent accuracy (<3.33%) and precision (<3.45%).

2.4. Pharmacokinetic analysis

2.4.1. Software

Concentration–time profiles were analysed through non-linear mixed-effects modelling by extended least-squares regression (Lindstrom and Bates, 1990), using the first-order estimation method. The NONMEM package (GloboMax LLC, Hanover, MD, USA) version V level 1.1 was used, with the NM-TRAN version III level 1 and PREDPP version IV level 1.0 (Beal et al., 1988–1998), installed on a PC Pentium IV platform. Compilations were achieved using the Microsoft Compact Visual Fortran (version 6.5.0). Graphical and other statistical analyses, including evaluation of NONMEM outputs, were performed using the S-Plus 6.1 Professional.

2.4.2. Structural pharmacokinetic model development

Previous analyses have demonstrated that salbutamol sulphate undergo efflux process from enterocyte to intestinal lumen mediated by transporters of the ATP-binding cassette family and, in particular, P-gp. Therefore, secretion process from enterocyte to intestinal lumen was always incorporated in the pharmacokinetic models and passive, active or combined (passive and active) kinetics for the absorption process of the salbutamol sulphate

was evaluated using three structural pharmacokinetic models, which are described as follows:

Model 1. First-order absorption and active secretion kinetics:

$$\frac{dL}{dt} = -k_a L + \frac{V'_{Max} E}{K'_m + E} \quad (2)$$

Model 2. Michaelis–Menten absorption and active secretion kinetics:

$$\frac{dL}{dt} = -\frac{V_{Max} L}{K_m + L} + \frac{V'_{Max} E}{K'_m + E} \quad (3)$$

Model 3. Combined first-order and Michaelis–Menten absorption and active secretion kinetics:

$$\frac{dL}{dt} = -k_a L - \frac{V_{Max} L}{K_m + L} + \frac{V'_{Max} E}{K'_m + E} \quad (4)$$

where L and E are the salbutamol sulphate concentrations at time t in the intestinal lumen and enterocyte, respectively; k_a the first-order absorption rate constant from intestinal lumen to enterocyte; V_{max} the maximal absorption rate from lumen to enterocyte, and K_m is the salbutamol sulphate concentration in the lumen at which the absorption rate is half-maximal; V'_{Max} the maximal secretion rate from enterocyte to the lumen, and K'_m is the salbutamol sulphate concentration in the enterocyte at which the secretion rate is half-maximal.

Due to initial membrane adsorption of the solute, sample dilution and/or presence of rapid metabolism, the calculated concentration at time 0 is usually lower than the initial concentration perfused (Sánchez-Picó et al., 1989). In order to overcome this effect, a correction fraction (FR) was introduced in the model to account for the fraction of initial concentration perfused available for the absorption from intestinal lumen to enterocyte. In addition, a dynamic equilibrium between intestinal lumen and enterocyte is achieved in the first five minutes (Doluisio et al., 1969). Consequently, E and L are proportional, and the use of L as representative of the enterocyte concentration is justified.

In the presence of competitive inhibitors of the active secretion processes, Eqs. (2)–(4) are expanded to Eqs. (5)–(7), respectively:

$$\frac{dL}{dt} = -k_a L + \frac{V'_{Max} E}{K'_m \left[1 + \frac{C}{IC_{50}}\right] + E} \quad (5)$$

$$\frac{dL}{dt} = - - \frac{V_{Max} L}{K_m + L} + \frac{V'_{Max} E}{K'_m \left[1 + \frac{C}{IC_{50}}\right] + E} \quad (6)$$

$$\frac{dL}{dt} = -k_a L - \frac{V_{Max} L}{K_m + L} + \frac{V'_{Max} E}{K'_m \left[1 + \frac{C}{IC_{50}}\right] + E} \quad (7)$$

where C is the concentration of the competitive inhibitor perfused, and IC_{50} is the concentration of the competitive inhibitor that produces a two-fold displacement in the apparent salbutamol sulphate K'_m value. In the particular case of the grapefruit juice, the real value of C is unknown. As a consequence, it was not possible to identify IC_{50} independently of the C value. Instead, an inhibition factor was estimated to quantify the grapefruit juice effect on salbutamol sulphate K'_m. At the value of the grapefruit juice concentration assessed, the inhibition factor (INF) is assumed to be equal to $1 + C/IC_{50}$.

Sodium azide inhibits the ATP productions by inhibiting the electron transport complexes in the mitochondrial matrix (Vasilyeva and Forgac, 1998). In the absence of ATP, the energy source for the active transport is missing and the carrier systems are blocked. The mechanism of action described for sodium azide is consistent with the mechanism of a non-competitive inhibition, where K'_m (and K_m, in models 2 and 3) remains constant, whereas V'_{Max} (and V_{Max}, in models 2 and 3) decreases as a function of the metabolic inhibitors concentrations. Therefore, in the presence of metabolic inhibitors with a direct effect on the active processes, Eqs. (5)–(7) are expanded to Eqs. (8)–(10), in order to reflect the structure of models 1, 2 and 3, respectively:

$$\frac{dL}{dt} = -k_a L + \frac{V'_{Max}\left[\frac{IM_{50}}{IM_{50}+M}\right] E}{K'_m \left[1 + \frac{C}{IC_{50}}\right] + E} \quad (8)$$

$$\frac{dL}{dt} = -\frac{V_{Max}\left[\frac{IM_{50}}{IM_{50}+M}\right] L}{K_m + L} + \frac{V'_{Max}\left[\frac{IM_{50}}{IM_{50}+M}\right] E}{K'_m \left[1 + \frac{C}{IC_{50}}\right] + E} \quad (9)$$

$$\frac{dL}{dt} = -k_a L - \frac{V_{Max}\left[\frac{IM_{50}}{IM_{50}+M}\right] L}{K_m + L} + \frac{V'_{Max}\left[\frac{IM_{50}}{IM_{50}+M}\right] E}{K'_m \left[1 + \frac{C}{IC_{50}}\right] + E} \quad (10)$$

where M represents the metabolic inhibitor concentration and IM_{50} is the metabolic inhibitor concentration that reduces 50% the V_{Max} and V'_{Max} values.

The underlying assumption of Eqs. (8)–(10) is that V'_{Max} (and V_{Max}, in models 2 and 3) was directly proportional to the amount of the ATP available in the enterocyte (Valenzuela, 2003). However, as the amount of ATP in the enterocyte was unknown, it was assumed that V'_{Max} (and V_{Max}, in models 2 and 3) was directly proportional to the ratio between available ATP concentration at time t and ATP concentration at time 0 in the enterocyte. Eq. (11) shows the relationships between V'_{Max} and ATP:

$$V'_{Max} = V'^{*}_{Max} \frac{[ATP]}{[ATP_0]} = V'^{*}_{Max}[ATP_R] \quad (11)$$

where, V'^{*}_{Max} is the maximal salbutamol sulphate secretion rate from enterocyte to lumen when the ATP concentration in the enterocyte, [ATP], is equal to the ATP concentration in the enterocyte at time 0, $[ATP_0]$. Similar equation was used for V_{Max} in models 2 and 3.

Since the depletion process of ATP in the enterocyte could not be an instantaneous process, an indirect response model (Dayneka et al., 1993) was used to describe the inhibitory effect of NaN_3 on the $[ATP_R]$ production rate (Eq. (12)):

$$\frac{dATP_R}{dt} = k_{In}\left(1 - \frac{M}{IM_{50} + M}\right) - k_{Out}[ATP_R] \quad (12)$$

where k_{In} and k_{Out} are the production and elimination rate constants of $[ATP_R]$, respectively, M represents the NaN_3 concen-

tration in the intestinal content, and IM_{50} represents the NaN_3 concentration, which inhibits $[ATP_R]$ production rate to 50%. In absence of NaN_3, the $[ATP_R]$ level remains constant and equal to 1. In this situation, k_{In} is equal to k_{Out}, and Eq. (12) can be rearranged as follows (Eq. (13)):

$$\frac{d[ATP_R]}{dt} = k_0 \left(\frac{IM_{50}}{IM_{50} + M} - [ATP_R] \right) \tag{13}$$

where k_0 is the rate constant that drives the delayed inhibition effect of V'_{Max} as a consequence of the direct effect of NaN_3 on the $[ATP_R]$ production in the enterocyte. Therefore, in the presence of metabolic inhibitors with an indirect effect on the active processes, Eqs. (5)–(7) are expanded to Eqs. (14)–(16), respectively:

$$\frac{dL}{dt} = -k_a L + \frac{V'^{*}_{Max}[ATP_R]E}{K'_m \left[1 + \frac{C}{IC_{50}}\right] + E} \tag{14}$$

$$\frac{dL}{dt} = -\frac{V^{*}_{Max}[ATP_R]L}{K_m + L} + \frac{V'^{*}_{Max}[ATP_R]E}{K'_m \left[1 + \frac{C}{IC_{50}}\right] + E} \tag{15}$$

$$\frac{dL}{dt} = -k_a L - \frac{V^{*}_{Max}[ATP_R]L}{K_m + L} + \frac{V'^{*}_{Max}[ATP_R]E}{K'_m \left[1 + \frac{C}{IC_{50}}\right] + E} \tag{16}$$

The magnitude of the residual random error in salbutamol sulphate concentrations was modelled using an exponential error model.

$$C_{obs} = C_{pred} \exp^{\varepsilon} \tag{17}$$

where C_{obs} is the ith observed concentration of salbutamol sulphate in the jth animal, C_{pred} the corresponding model predicted concentration, ε the independent normally distributed random variables with zero mean and variances, σ^2, which describes the residual departure of the observed concentration from the model predicted concentration. Due to rather limited variability in the experimental data, interindividual random effects were not included in the model at this stage.

For hierarchical models, the improvement in the fit obtained through the inclusion of a fixed effect into the overall model was assessed using the likelihood ratio test (LRT). LRT is a statistic based on the change in the minimum value of the objective function (ΔMVOF), which is proportional (up to a constant) to minus twice the log-likelihood of the data and is asymptotically distributed like χ^2 with the degrees of freedom equal to the number of parameters added to the model. A change in MVOF of 3.84 was required to reach statistical significance at $p \leq 0.05$ for the addition of one fixed effect. The magnitude of the residual variability, the precision of the parameter estimate and the examination of the scatterplots of weighted residuals against predicted concentrations and time were also evaluated to select the optimal structural absorption model.

2.4.3. Interindividual random effects model

Interindividual variability (IIV) was initially assumed for all pharmacokinetic parameters and was implemented as a diagonal variance matrix for random effects. Individual values of all pharmacokinetic parameters were assumed to follow the log-normal distribution, which was implemented as follows:

$$P_j = P^* \exp^{\eta_{P_j}} \tag{18}$$

where P_j is an individual pharmacokinetic parameter for the jth individual, P^* the typical value of the pharmacokinetic parameter and η_{P_j} is a normally distributed random variable with zero-mean and variance ω^2_P, that distinguishes the jth individuals' pharmacokinetic parameter from the population typical value, P^*. The magnitude of IIV in the pharmacokinetic parameters was expressed as a coefficient of variation (CV).

After fitting the mixed-effect model, the interindividual random effects that turned out to be not estimable were fixed to zero. Then, the distributions of the estimable random effects were graphically examined to evaluate the normality assumption. Also, each random effect was also plotted against all other random effects in order to explore the correlations. The random effects with the highest correlations were tested by including the corresponding non-diagonal element in the matrix of random effects. If the implementation of a correlation between random effects significantly improved the fit, the off-diagonal element in the matrix of random effects was kept in the model and the process was repeated until no further improvement of the fit could be achieved. At this stage, the final population absorption model was obtained.

2.4.4. Model evaluation

A parametric and non-parametric bootstrap analysis was performed as an internal model evaluation technique, using the package Wings for NONMEM (N. Holford, Version 4.04, June 2003, Auckland, New Zealand). For the non-parametric bootstrap, a new replication of the original dataset (a bootstrap sample) was obtained by N random draws of individual animal data (with replacement) from the original dataset. For the parametric bootstrap, a new replication of the dataset (a bootstrap sample) was obtained by simulating the individual animal data from the original dataset using the final pharmacokinetic model. The final population pharmacokinetic model was re-fitted to each new dataset and this process was repeated 1000 times with different random draws for the parametric and non-parametric bootstrap. The stability of the final model was evaluated by visual inspection of the distribution of the model parameter estimates from the new datasets and compared with that obtained from the fit of the original dataset (Efron and Tibshirani, 1993). Bootstrap runs with unsuccessful minimization were excluded from further analysis. The final model parameter estimates were compared to the mean and 95% confidence intervals of the parametric and non-parametric bootstrap replicates of the final model.

3. Results

Six-hundred and twenty-four salbutamol sulphate concentrations corresponding to 104 Wistar rats (six concentrations per rat) were used in this analysis. In total, 43 models of varying complexities were subsequently tested to evaluate the salbu-

Table 1
Description of the model selection process to quantify the salbutamol sulphate absorption

Model	Absorption model[a]	ATP inhibition	Reference model	Degree of freedom	ΔMVOF	*p*-Value
1	Pasive[b]	Direct	–	–	–	–
2	Active	Direct	1	1	−28.43	<0.001
3	Combined	Direct	2	1	−46.40	<0.001
4	Pasive	Indirect	1	1	−3.03	0.082
5	Active	Indirect	2	1	−12.13	<0.001
6	Combined	Indirect	3	1	−0.17	0.680

[a] Passive absorption was characterized by first-order absorption. Active absorption was characterized by Michaelis–Menten absorption. Combined was characterized by a simultaneous passive and active absorption.
[b] MVOF = −3503.116.

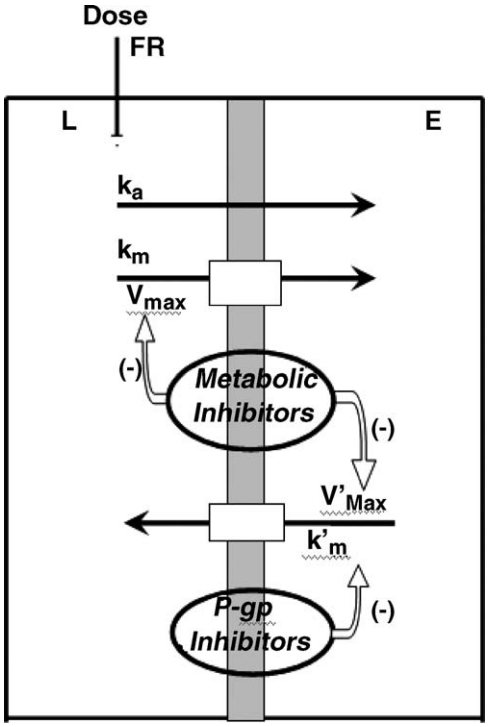

Fig. 1. Schematic of the salbutamol sulphate model.

tamol sulphate absorption in rat small intestine. The model selection process is summarized in Table 1 and a scheme of the final model is represented in Fig. 1. The first-order absorption model successfully fitted the data. Substantial further improvement of the fit was achieved by considering a Michaelis–Menten absorption or a combined passive diffusion and active absorption processes from lumen to enterocyte. Consequently, when an instantaneous dynamic equilibrium in salbutamol sulphate concentrations is achieved between luminal and enterocyte, the salbutamol sulphate absorption process was best described by a combined passive diffusion and active absorption processes from intestinal lumen to enterocyte, simultaneous to an active capacity-limited efflux from enterocyte to intestinal lumen.

The effect of P-gp inhibitors was well characterized with a competitive agonism model on the active secretion process from enterocyte to intestinal lumen. Not statistical significant differences were found between direct (model 3) and indirect (model 6) mechanisms of the NaN_3 inhibitory effect (Table 1), when passive and combined absorption models were compared. However, statistical significant differences were found between direct and indirect mechanism when active absorption model was combined. Diagnostic plots of models 3 and 6 showed random, uniform scatter around the identity line and indicated an absence of bias in this model (data not shown). As a consequence models 3 and 6 were selected to evaluate the inclusion of interindividual random effects.

Only interindividual random effects on k_a and FR were identifiable, consequently all other effects were fixed to zero. Further hypothesis testing revealed that the correlation between k_a and FR random effects was not different from 1, and therefore was fixed to 1. Tables 2 and 3 show the population pharmacokinetic estimates parameters of the salbutamol sulphate for the models 3 and 6, respectively. Based on the parsimony principle, model 3 was selected as the final population pharmacokinetic model for salbutamol sulphate absorption in rat small intestine. Observed salbutamol sulphate concentrations and individual and population model predictions versus time in absence or presence of grapefruit juice, verapamil and NaN_3 are displayed in Figs. 2 and 3, respectively. Diagnostic plots are presented in Fig. 4 and showed random, uniform scatter around the line of identity and suggested the absence of any trend or bias, while histogram of individual random effect showed approximately normal distribution (data not shown). These plots clearly demonstrated the adequacy of the final population pharmacokinetic model to describe the absorption of salbutamol sulphate in rats after the in situ administration.

Nonparametric and parametric bootstrap analyses were used as internal model evaluation techniques to qualify the salbutamol sulphate absorption model. The results of both analyses are presented in Tables 2 and 3 for models 3 and 6, respectively. From the 1000 replicates of model 3, 20.8 and 3.3% failed to minimize successfully in the non-parametric and parametric bootstrap, respectively. From the 1000 replicates of model 6, 41.3 and 37.5% failed to minimize successfully in the non-parametric and parametric bootstrap, respectively. In both models, the population estimates for the final model were similar to the mean of the non-parametric and parametric bootstrap replicates, respectively, and were contained within the 95% confidence intervals obtained from the both bootstrap analyse. The precision of the NONMEM parameter estimates was also acceptable as derived from the 95% confidence intervals of Tables 2 and 3. These findings suggested a high accuracy of the NONMEM parameter

Table 2
Population pharmacokinetic parameters of salbutamol sulphate from in situ data in rats and the stability of the model parameters using non-parametric and parametric bootstraps (model 3)

Model parameters	Original dataset	Non-parametric bootstrap ($N=792$ replicates)			Parametric bootstrap ($N=967$ replicates)		
	Estimate	Mean	95% CI lower limit	95% CI upper limit	Mean	95% CI lower limit	95% CI upper limit
Structural model							
FR (%)	79.5	79.5	78.5	80.5	79.1	78.1	80.1
k_a (h^{-1})	0.636	0.630	0.606	0.654	0.636	0.612	0.660
V_{Max} (mM/h)[a]	0.726	0.936	0.330	2.310	0.785	0.366	1.452
K_m (mM)[a]	0.540	0.710	0.202	1.744	0.582	0.221	1.170
V'_{Max} (mM/h)[a]	0.678	0.816	0.378	1.806	0.712	0.402	1.182
K'_m (mM)[a]	0.357	0.445	0.162	1.042	0.370	0.170	0.679
ID_{50} (mM)	7.330	7.889	3.128	15.60	7.510	4.080	12.600
INF	1.450	1.465	1.260	1.780	1.470	1.290	1.690
IM_{50} (mM)	0.077	0.072	0.016	0.142	0.080	0.001	0.197
Interindividual variability (%)							
η_{K_a}	7.80	7.57	5.91	9.05	7.45	5.85	8.94
η_{FR}	28.00	27.68	23.07	32.55	27.32	23.44	31.33
Residual variability (%)							
Exponential error	1.03	1.03	0.89	1.20	1.03	0.96	1.10

Correlation between ka and FR is set to 1.
[a] Units referred to salbutamol sulphate concetrations.

Table 3
Population pharmacokinetic parameters of salbutamol sulphate from in situ data in rats and the stability of the model parameters using non-parametric and parametric bootstraps (model 6)

Model parameters	Original dataset	Non-parametric bootstrap ($N=587$ replicates)			Parametric bootstrap ($N=625$ replicates)		
	Estimate	Mean	95% CI lower limit	95% CI upper limit	Mean	95% CI lower limit	95% CI upper limit
Structural model							
FR (%)	79.3	79.3	78.3	80.3	78.9	78.0	79.8
k_a (1/h)	0.636	0.639	0.616	0.666	0.639	0.612	0.666
V_{Max} (mM/h)[a]	0.678	0.734	0.323	1.550	0.692	0.325	1.320
K_m (mM)[a]	0.494	0.528	0.207	1.143	0.505	0.192	1.032
k_0 (1/h)	18.96	18.00	9.40	36.54	16.22	7.49	28.14
V'_{Max} (mM/h)[a]	0.642	0.687	0.367	1.290	0.649	0.374	1.134
K'_m (mM)[a]	0.333	0.351	0.158	0.678	0.336	0.149	0.630
ID_{50} (mM)	7.13	7.48	3.05	14.4	7.02	3.57	11.58
INF	1.46	1.49	1.28	1.82	1.49	1.32	1.77
IM_{50} (mM)	0.074	0.075	0.025	0.134	0.072	0.00	0.183
Interindividual variability (%)							
η_{K_a}	7.82	7.46	5.94	8.84	7.33	5.81	8.86
η_{FR}	27.8	27.6	22.8	32.6	26.9	23.1	30.7
Residual variability (%)							
Exponential error	1.03	1.01	0.88	1.12	1.03	0.96	1.10

Correlation between ka and FR is set to 1.
[a] Units referred to salbutamol sulphate concetrations.

estimates for both models, and confirmed that the current study design supports the estimation of model parameters for model 3 but not for model 6.

4. Discussion

Rat has been widely used as an animal model to project the intestinal permeability in humans and to investigate the mechanism of intestinal transport of drugs by in situ and in vivo experimental studies (Chiou and Barve, 1998). Human perfusion studies have demonstrated an excellent correlation between intestinal permeability of the both species for a variety of compounds (Amidon et al., 1995). In this study, a rat model and Doluisio techniques were selected to investigate the absorption process and the intestinal transport characteristics of salbutamol sulphate over an extensive range of concentrations. In order to detect non-linearities in the absorption process, a 120-fold range of concentrations was covered with seven different concentration levels ranging from 0.15 to 18 mM, including concentrations well beyond the allometric dose of salbutamol sulphate in rat.

The stability of salbutamol sulphate in the intestinal media was checked to unequivocally ascribe the losses to the absorption

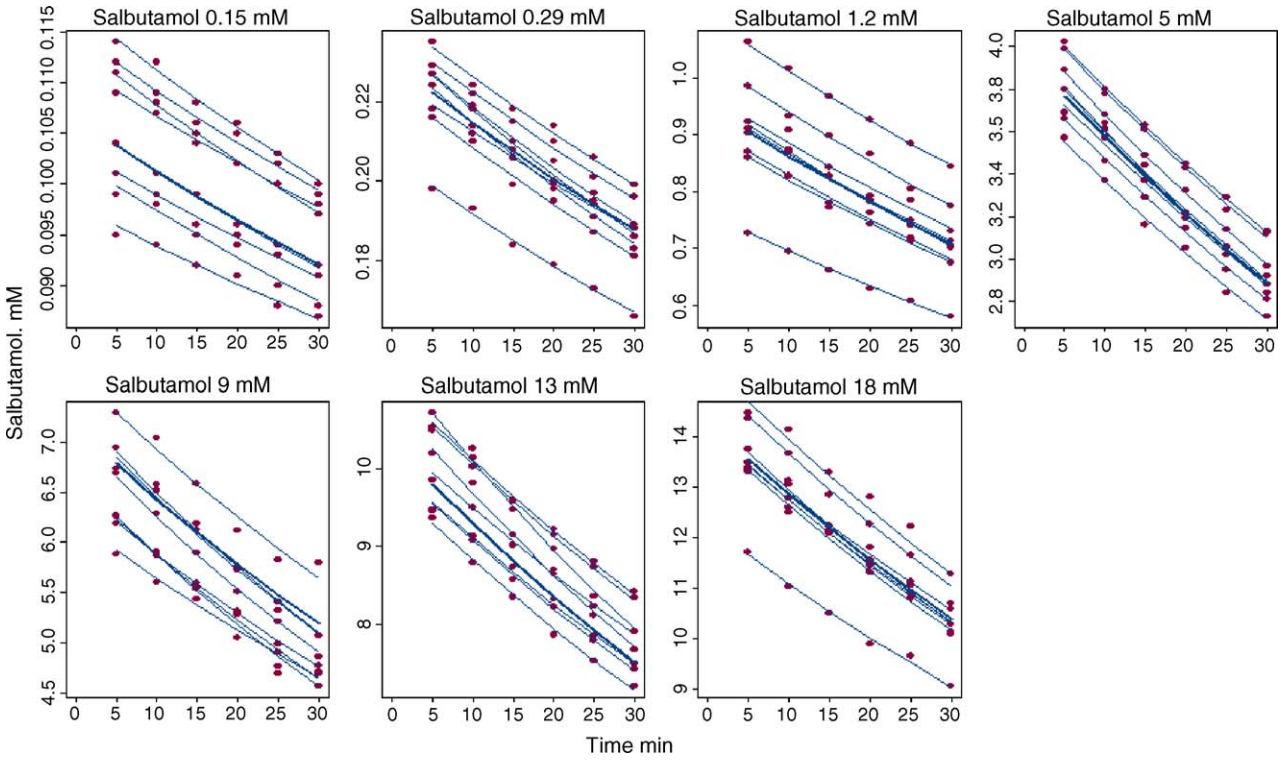

Fig. 2. Observed salbutamol sulphate concentrations (circles) and individual (lines) and population (bold line) model predictions vs. time in absence of inhibitors. Salbutamol refers to salbutamol sulphate.

process (Valenzuela et al., 2001). However, a correction fraction (FR) was introduced in the model to account for the fraction of initial concentration perfused available for the absorption from intestinal lumen to enterocyte. Process such as initial membrane adsorption of the solute, sample dilution and/or presence of rapid luminal metabolism of salbutamol sulphate, can produce that the calculated concentration at time 0 is usually lower than the initial concentration perfused.

The role of active secretion from enterocyte to intestinal lumen, mediated by P-gp efflux pump, was studied by performing salbutamol sulphate absorption studies in presence of metabolic inhibitors (NaN_3) and P-gp inhibitors (verapamil and

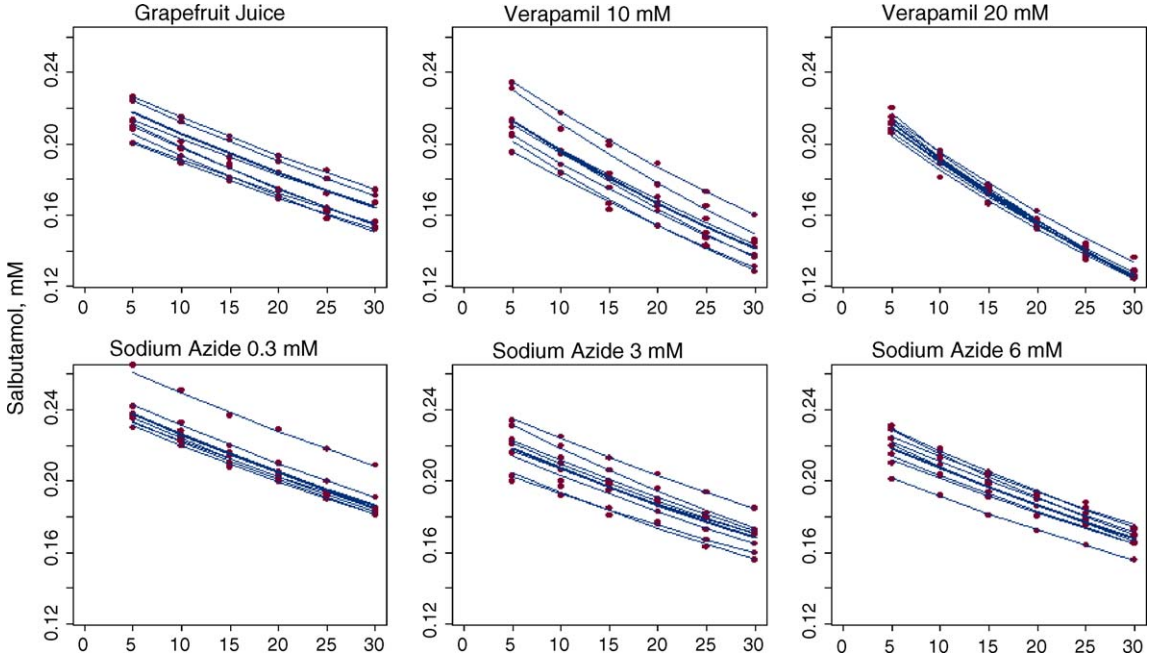

Fig. 3. Observed salbutamol sulphate concentrations (circles) and individual (lines) and population (bold line) model predictions vs. time in presence of inhibitors. Salbutamol refers to salbutamol sulphate.

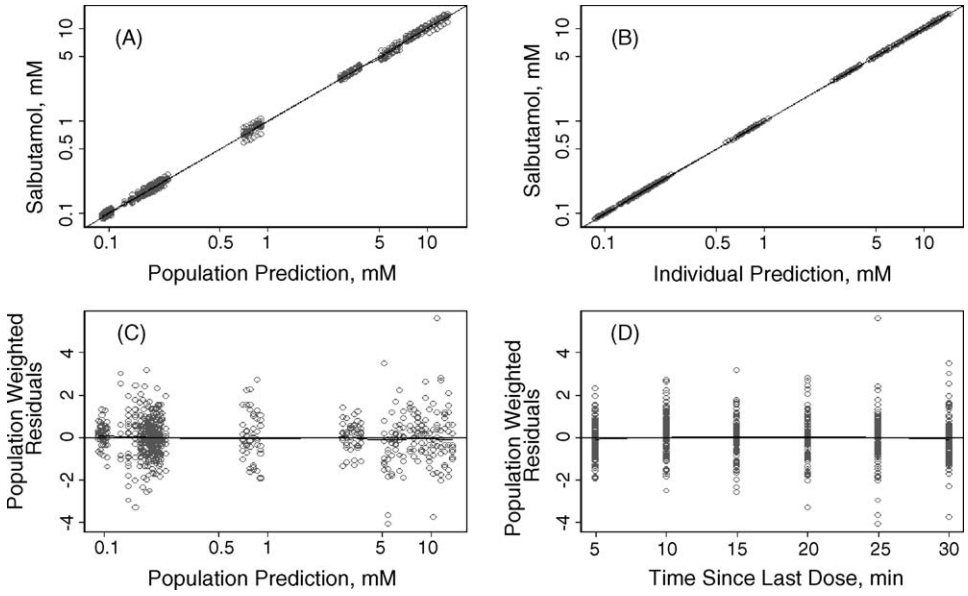

Fig. 4. Goodness of fit plots for the final model: scatter plots of the observed salbutamol sulphate concentrations vs. the population model predictions (A) and the individual model predictions (B), scatter plots of the population weighted residuals vs. the population model predictions (C) and time (D). Salbutamol refers to salbutamol sulphate.

grapefruit juice). This complex experimental design covered different conditions, which were integrated all together in order to properly identify and characterize the potential sources of nonlinearity in the absorption process of salbutamol sulphate.

Population pharmacokinetic approach using NONMEM has been widely employed to investigate pharmacokinetics processes using data from in situ studies in rats (Fernandez-Teruel et al., 2005; Leal et al., 2005; Muñoz et al., 2005). Using this approach, the model selection process suggested that salbutamol sulphate absorption was best described by a combined passive diffusion and active absorption processes from intestinal lumen to enterocyte, with an active capacity-limited efflux from enterocyte to intestinal lumen. The evidence of the salbutamol sulphate active secretion process along the whole length of the rat small intestine is mediated by P-gp, has been reported previously in two articles (Valenzuela et al., 2001; Valenzuela et al., 2004). However, to the best of our knowledge no evidence of combined passive diffusion and active absorption processes has been reported up to date. This mechanism of absorption suggests the involvement of ATP in the salbutamol sulphate absorption and hence it supports the existence of an active carrier-mediated process. Recently, it was suggested that OCT family is involved in bronchoephitelial salbutamol transport (Ehrhardt et al., 2005). Examination of tissue distribution of the OCT family also indicates that OCT1 and OCT3 are expressed in the small intestine of rats (Katsura and Iuni, 2003). Therefore, OCT transporters could be involved in the salbutamol absorption in rats.

The model described above assumed that salbutamol sulphate concentrations in the enterocyte and the intestinal lumen were in dynamic equilibrium after 5 min and, therefore, salbutamol sulphate concentration in the enterocyte were assumed to be proportional to the salbutamol sulphate concentrations in the intestinal lumen. This phenomenon has been described frequently when in situ studies are used to investigate the drug absorption process (Ruíz-Balaguer et al., 1997; Rodríguez-Ibáñez et al., 2003; Muñoz et al., 2005). In order to evaluate this assumption, a non-instantaneous equilibrium between enterocyte and intestinal lumen was tested. The non-instantaneous equilibrium model did not provide substantial improvement of the fit relative to an instantaneous equilibrium model.

The effect of P-gp inhibitors was well characterized with a competitive agonism model on the active secretion process from enterocyte to intestinal lumen. The data available did not allow discriminating between a direct (model 3) and indirect (model 6) mechanism of the inhibitory effect of NaN_3. Also, an exhaustive literature review failed to find any paper that supports or detracts the direct or indirect inhibitory mechanism of the inhibitory effect of NaN_3. The depletion model of ATP in presence of sodium azide was published first by Valenzuela (Valenzuela, 2003) and, later on used to quantify the sarafloxacin absorption process from in situ data (Fernandez-Teruel et al., 2005). In both cases, the value of k_0 obtained was similar to the results obtained in the present paper ($18.96\,h^{-1}$). The half-life associated with k_0 was shorter than 5 min, the time to collect the first sample. It reflects a relatively fast process to achieve a dynamic equilibrium between drug concentration in the intestinal lumen and the enterocyte. In this situation, model 6 collapses to model 3. In addition, parametric bootstrap demonstrated that the study design was not good enough to fully characterize the model 6 because approximately 37.5% of the parametric bootstrap replicates failed to get convergence. It is probably due to the overparameterization of model 6 and/or the relative fast inhibition process mediated by sodium azide. For all these reasons, model 3 was selected as the final salbutamol sulphate absorption process in rat small intestine.

The model developed did not consider the effect on NaN_3 on the salbutamol passive absorption pathway. However, high concentration of NaN_3 could affect the overall enterocyte mem-

brane integrity. As a consequence the paracellular absorption of salbutamol would increase. In order to evaluate this hypothesis, the current final model was modified to account for the potential effect of NaN_3 on the first-order absorption rate from intestinal lumen to enterocyte according to Eq. (19):

$$k_a = k_a^* \left(1 + \frac{k_{max} M}{SM_{50} + M}\right) \quad (19)$$

where, k_a is the first-order absorption rate from intestinal lumen to enterocyte; k_a^* the first-order absorption rate from intestinal lumen to enterocyte in absence of NaN_3; k_{max} the maximal k_a^* increase in presence of NaN_3 (M) and SM_{50} is the sodium azide concentration at which the k_a^* increase half-maximal. The magnitude of the NaN_3 effect on the paracellular absorption process was negligible as the maximal increase in the absorption rate was lower than 0.01%. Furthermore, statistical analysis evidenced that the modified model did not significantly improve the goodness-of-fit. Therefore, the data available did not support the enhancement of paracellular absorption of salbutamol in presence of NaN_3.

The reliability of the results obtained from population pharmacokinetic analyses were explored through the model evaluation process. In the absence of a new data set, parametric and non-parametric bootstrap techniques are two of the internal evaluation methods that may be especially useful for this purpose (Ette, 1997). Both bootstrap analyses conducted in the current study, yielded mean model parameters that were comparable to the estimates of the original data set, indicating the stability of the developed model and supporting the study design for parameter estimation of model 3.

According to the final pharmacokinetic model, Table 2 shows that salbutamol sulphate has higher affinity and lower capacity for the secretion process ($K'_m = 0.357$ mM, $V'_{Max} = 0.678$ mM/h) than active absorption process ($K_m = 0.540$ mM, $V_{Max} = 0.726$ mM/h). Considering the contribution of the passive diffusion ($0.636\ h^{-1}$) to the global salbutamol sulphate absorption process, in average, the absorption rate is faster than the secretion rate over the entire range of salbutamol sulphate concentrations studied. In fact, the difference in the absorption and secretion rates (net absorption) increased with salbutamol sulphate concentrations. Therefore, the yield of the net absorption process increase at higher concentrations, and it is optimal at concentrations higher than 10 mM, where the secretion process is completely saturated (Fig. 5). However, it's very unlikely to have similar concentrations in the clinical setting as 10 mM is a 30-fold higher dose than the allometric dose of salbutamol in rat.

In presence of grapefruit juice, verapamil at concentrations of 10 and 20 mM, the K'_m values were shifted to 0.52, 0.84 and 1.33 mM, respectively (Fig. 5). Therefore, the presence of P-gp competitive inhibitors increases the amount of salbutamol sulphate in the enterocyte. The extent of this effect is higher for verapamil 20 mM and lower for grapefruit juice. In presence of NaN_3 at concentrations of 0.3, 3 and 6 mM, the maximum capacity of the active absorption and secretion is reduced by 79.58, 97.50 and 98.53%, respectively. These values are well above 50% inhibition, which is translated into a poor precision of IM_{50} estimate as no data from concentrations inhibiting ATP-synthetase by less than 50% were available. Based on the point estimates, the salbutamol sulphate absorption in presence of NaN_3 concentrations equal or higher than 3 mM is characterized by a first-order absorption with an approximate absorption rate constant of $0.636\ h^{-1}$, which yield a net absorption rate very similar relative to the presence of grapefruit juice (range: 0.636–$0.671\ h^{-1}$), but in the low range of apparent absorption rate constant observed in presence of verapamil 10 mM (range: 0.636–$1.162\ h^{-1}$) and 20 mM (range: 0.636–$1.450\ h^{-1}$) over a range of salbutamol sulphate concentration from 0.01 to 20 mM. Based on these results, the extent of salbutamol sulphate absorption in rat small intestine can be improved by NaN_3 0.3, 3 and 6 mM, grapefruit juice and verapamil 10 and 20 mM, in ascending order.

In summary, the population approach has been used to integrate the pharmacokinetic knowledge gathered from preclinical

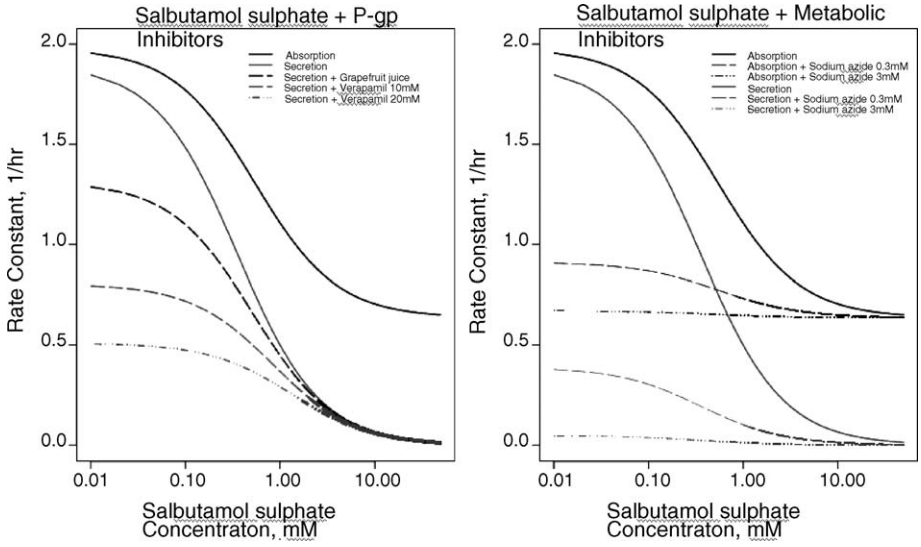

Fig. 5. Effect of P-gp (left) and metabolic (right) inhibitors on the salbutamol sulphate rate constants.

studies. The model developed was suitable to describe the complex salbutamol sulphate absorption in rat small intestine and characterized the effect of NaN_3, grapefruit juice and verapamil.

References

Ahrens, R.C., Smith, G.D., 1984. Albuterol: an adrenergic agent for use in the treatment of asthma pharmacology, pharmacokinetics and clinical use. Pharmacotherapy 4, 105–121.

Amidon, G.L., Lennernas, H., Shah, V.P., Crison, J.R., 1995. A theoretical basis for a biopharmaceutic drug classification: the correlation of in vitro drug product dissolution and in vivo bioavailability. Pharm. Res. 12, 413–420.

Beal, S.L., Boeckmann, A., Sheiner, L.B., 1988–1998. NONMEM users guides. Part I–VIII, NONMEM Project Group C2555. University of California at San Francisco, San Francisco.

Chiou, W.L., Barve, A., 1998. Linear correlation of the fraction of oral dose absorbed of 64 drugs between humans and rats. Pharm. Res. 21, 217–223.

Dayneka, N.L., Garg, V., Jusko, W.J., 1993. Comparison of four basic models of indirect pharmacodynamic responses. J. Pharmacokinet. Biopharm. 21, 457–478.

Doluisio, J.T., Billups, N.F., Dittert, L.W., Sugita, E.T., Swintosky, J.V., 1969. Drug absorption. Part I. An in situ rat gut technique yielding realistic absorption rates. J. Pharm. Sci. 56, 1196–1200.

Edwards, D.J., Bellevue III, F.H., Woster, P.M., 1996. Identification of 6′,7′-dihidroxybergamottin, a cytochrome P450 inhibitor, in grapefruit juice. Drug. Metab. Dispos. 24, 1287–1290.

Ehrhardt, C., Kneuer, C., Bies, C., Lehr, C.M., Kim, K.J., Bakowsky, U., 2005. Salbutamol is actively absorbed across human bronchial epithelial cell layers. Pulm. Pharmacol. Ther. 18, 165–170.

Efron, B., Tibshirani, R., 1993. An Introduction to the Bootstrap. Chapman & Hall, London, UK.

Ette, E.I., 1997. Stability and performance of a population pharmacokinetic model. J. Clin. Pharmacol. 37, 486–495.

Fernandez-Teruel, C., Gonzalez-Alvarez, I., Casabo, V.G., Ruiz-Garcia, A., Bermejo, M., 2005. Kinetic modelling of the intestinal transport of sarafloxacin. Studies in situ in rat and in vitro in Caco-2 cells. J. Drug Target 13, 199–212.

Gabús-Sannié, C., Buri, P., 1987. Étude comparative des méthodes de détermitation du volume d'eau absorbé lors de perfusion de l'íntestine grêle du rat. S.T.P. Pharma 3, 856–860.

Katsura, T., Iuni, K., 2003. Intestinal absorption of drugs mediated by drug transporters: mechanisms and regulation. Drug Metab. Pharmacokin. 18, 1–15.

Leal, N., Calvo, R., Agrad, F.Z., Lukas, J.C., de la Fuente, L., Suarez, E., 2005. Altered dose-to-effect of propofol due to pharmacokinetics in rats with experimental diabetes mellitus. J. Pharm. Pharmacol. 57, 317–325.

Legen, I., Žakelj, S., Kristl, A., 2003. Polarised transport of monocarboxylic acid type drugs across rat jejunum in vitro: the effect of mucolysis and ATP-depletion. Int. J. Pharm. 256, 161–166.

Lindstrom, M.J., Bates, T.M., 1990. Nonlinear mixed effects models for repeated measures. Biometrics 46, 673–687.

Martín-Villodre, A., Plá-Delfina, J.M., Moreno-Dalmau, J., Pérez-Buendía, M.D., Miralles, J., Collado, E., Sánchez-Moyano, E., Del Pozo, A., 1986. Studies on the reliability of a bihyperbolic functional absorption model. Part I. Ring substituted anilines. J. Pharmacokinet. Biopharm. 14, 615–633.

Muñoz, M.J., Merino-Sanjuan, M., Lledó-García, R., Casabó, V.G., Mañez-Castillejo, F.J., Nácher, A., 2005. Use of nonlinear mixed effect modeling for the intestinal absorption data: application to ritonavir in the rat. Eur. J. Pharm. Biopharm. 61, 20–26.

Pacifici, G.M., Giulianetti, B., Quilici, M.C., Spisni, R., Nervi, M., Giuliani, L., Gomeni, R., 1997. (−)-salbutamol sulphate sulphation in the human liver and duodenal mucosa: interindividual variability. Xenobiotica 27, 279–286.

Parker, T.J., Della Pasqua, O.E., Loizillon, E., Chezaubernard, C., Jochemsen, R., Danhof, M., 2001. Pharmacokinetic–pharmacodynamic modelling in the early development phase of anti-psychotics: a comparison of the effects of clozapine, S 16924 and S 18327 in the EEG model in rats. Br. J. Pharmacol. 132, 151–158.

Rodríguez-Ibáñez, M., Nalda-Molina, R., Montalar-Montero, M., Bermejo, M.V., Merino, V., Garrigues, T.M., 2003. Transintestinal secretion of ciprofloxacin, grepafloxacin and sparfloxacin: in vitro and in situ inhibition studies. Eur. J. Pharm. Biopharm. 55, 241–246.

Ruíz-Balaguer, N., Nácher, A., Casabó, V.G., Merino, M., 1997. Nonlinear intestinal absorption kinetics of cefuroxime axetil in rats. Antimicrob. Agents Chemother. 41, 445–448.

Ruíz-Balaguer, N., Nácher, A., Casabó, V.G., Merino-Sanjuán, M., 2002. Intestinal transport of cefuroxime axetil in rats: absorption and hydrolysis processes. Int. J. Pharm. 234, 101–111.

Sánchez-Picó, A., Peris-Ribera, J.E., Toledano, C., Torres-Molina, F., Casabó, V.G., Martín-Vilodre, A., Plá-Delfina, J.M., 1989. Nonlinear intestinal absorption kinetics of cefadroxil in the rat. J. Pharm. Pharmacol. 41, 179–185.

Sancho-Chust, V., Bengoechea, M., Fabra-Campos, S., Casabó, V.G., Martínez-Cámara, M.J., Martín-Villodre, A., 1995. Experimental studies on the influence of surfactants on intestinal absorption of drugs. Cefadroxil as model drug and sodium laurylsulfate as model surfactant: studies in rat duodenum. Arzneimittelforschung 45, 1013–1017.

Shono, Y., Nishihara, H., Matsuda, Y., Furukawa, S., Okada, N., Fujita, T., Yamamoto, A., 2004. Modulation of intestinal P-glycoprotein function by Cremophor EL and other surfactants by an in vitro difusion chamber method using the isolated rat intestinal membranes. J. Pharm. Sci. 93, 877–885.

Tanakaga, H., Ohnishi, A., Matsuo, H., Sawada, Y., 1998. Inhibition of vinblastine efflux mediated by P-glycoprotein by grapefuit juice components in Caco-2 cells. Biol. Pharm. Bull. 21, 1062–1066.

Tsuruo, T., Iida, H., Tsukagoshi, S., Sakurai, Y., 1981. Overcoming of vincristine resistance in P388 leukemia in vivo and in vitro through enhanced cytotoxicity of vincristine and vinblastine by verapamil. Cancer Res. 41, 1967–1972.

Tunblad, K., Hammarlund-Udenaes, M., Jonsson, E.N., 2005. Influence of probenecid on the delivery of morphine-6-glucuronide to the brain. Eur. J. Pharm. Sci. 24, 49–57.

Valenzuela, B., Nácher, A., Casabó, V.G., Martín-Villodre, A., 2001. The influence of active secretion processes on intestinal absorption of salbutamol sulphate in the rat. Eur. J. Pharm. Biopharm. 52, 31–37.

Valenzuela, B., 2003. Absorción del salbutamol sulphate: Estudios "in situ" e "in vivo". Influencia de los procesos de secreción. Ph.D. Thesis, University of Valencia, Spain.

Valenzuela, B., Nácher, A., Ruiz-Carretero, P., Martín-Villodre, A., López-Carballo, G., Barettino, D., 2004. Profile of P-glycoprotein distribution in the rat and its possible influence on the salbutamol sulphate intestinal absorption process. J. Pharm. Sci. 93, 1641–1648.

Varma, M.V.S., Ashokraj, Y., Dey, C.S., Panchagnula, R., 2003. P-glycoprotein inhibitors and their screening: a perspective from bioavailability enhancement. Pharmacol. Res. 48, 347–359.

Vasilyeva, E., Forgac, M., 1998. Interaction of the clathrin-coated vesicle V-ATPase with ADP and sodium azide. J. Biol. Chem. 273, 23823–23829.

Williams, P.J., Ette, E.I., 2000. The role of population pharmacokinetics in drug development in light of the Food and Drug Administration's 'Guidance for industry: population pharmacokinetics'. Clin. Pharmacokinet. 39, 385–395.

Woodland, C., Koren, G., Wainer, I.W., Batist, G., Ito, S., 2003. Verapamil metabolites: potential P-glycoprotein-mediated multidrug resistance reversal agents. Can. J. Physiol. Pharmacol. 81, 800–805.